SUPPLEMENTARY

Supplementary Summary (Acute vs. Chronic stage, CVI and vessel plexus changes):

In the acute stage of NAION, the vessel density (VD) of the intermediate capillary plexus (ICP) in the VF defect regions was significantly increased compared with healthy control (HC) (adjusted $P < 0.0001$). However, the choroidal vascularity index (CVI) did not show significant differences between the VF defect and controls ($P > 0.05$), indicating that choroidal vascular remodeling is not a dominant feature during the acute ischemic phase.

In contrast, in the chronic stage, VD reduction persisted in the radial peripapillary capillary plexus (RPCP), superficial vascular plexus (SVP) and ICP (RPCP, *adj-P* < 0.0001; SVP, *adj-P* = 0.003; ICP, *adj-P* = 0.004) in VF defect regions compared with HC, whereas both the VF defect and unaffected regions showed significantly higher CVI values compared with controls (defect vs. HC: *adj-P* = 0.04; unaffected vs. HC: *adj-P* < 0.0001). These findings suggest that choroidal vascularity index elevation is a characteristic of the chronic phase rather than the acute stage, possibly reflecting long-term vascular remodeling or compensatory dilation in response to chronic ischemic damage (Supplementary Table S1).

Supplementary Table S1 Wide-filed SS-OCTA inner VD and CVI for VF defected and VF unaffected regions in NAION-affected eyes

Characteristic Acute stage	HC matched region (*n* = 20)	Acute VF defect region* (*n* = 22)	Acute VF unaffected region# (*n* = 22)	*H/P*	defect vs. HC *adj-P*	unaffected vs. HC *adj-P*	defect vs. unaffected *adj-P*
RPCP	33.42[29.76,34.11	37.59[30.13,39.16]	32.69[31.12,34.14]	6.14 **0.046***	0.05	0.24	0.99
SVP	31.37[29.11,32.32]	32.62[26.55,32.79]	30.37[29.33,32.77]	0.26 0.89	0.62	0.82	0.80
ICP	25.21[24.38,27.18]	28.84[25.66,31.26]	27.52[24.97,29.58]	11.30 **0.004****	**0.003****	0.07	0.88
DCP	16.25[15.99,18.41]	18.24[17.60,19.49]	16.72[9.88,17.12]	14.48	0.11	0.31	**0.0004*****

Characteristic Acute stage	HC matched region (*n* = 20)	Acute VF defect region* (*n* = 22)	Acute VF unaffected region# (*n* = 22)	*H/P*	defect vs. HC *adj-P*	unaffected vs. HC *adj-P*	defect vs. unaffected *adj-P*
CVI	0.31[0.30,0.32]	0.31[0.29,0.35]	0.35[0.32,0.41]	**0.001**** 11.58 **0.003****	1.000	**0.003****	**0.04***
Characteristic Chronic stage	HC matched region (*n* = 20)	Chronic VF defect region* (*n* = 27)	Chronic VF unaffected region# (*n* = 27)	H/P	defect vs. HC *adj-P*	unaffected vs. HC *adj-P*	defect vs. unaffected *adj-P*
RPCP	33.42[29.76,34.11]	23.90[18.80,25.55]	27.03[21.67,31.42]	20.97 **<** **0.0001******	**<** **0.0001******	**0.03***	0.09
SVP	31.37[29.11,32.32]	21.89[20.88,23.86]	28.24[23.14,30.90]	16.68 **0.0002*****	**0.003****	1.000	**0.001****
ICP	25.21[24.38,27.18]	20.36[19.09,22.79]	22.95[19.71,25.42]	10.45 **0.005****	**0.004****	0.43	0.18
DCP	16.25[15.99,18.41]	19.90[18.22,21.99]	15.86[11.27,19.15]	8,28 **0.02***	0.14	0.99	**0.02***
CVI	0.31[0.30,0.32]	0.34[0.30,0.36]	0.36[0.33,0.40]	19.30 **<** **0.0001******	**0.04***	**< 0.0001******	0.12

VF defect = region with perimetric loss; # VF unaffected = region without perimetric loss.

Values are median [IQR]. Kruskal–Wallis with Dunn's post hoc test [Bonferroni correction].

*adj-*P* < 0.05, **adj-*P* < 0.01, ***adj-*P* < 0.001, ****adj-*P* < 0.0001.

Supplementary Vessel Density Analysis and Functional Correlation

To clarify the apparent discrepancy between our findings of peripapillary vessel density (ppVD) elevation and previous reports of VD reduction in acute NAION, we performed a set of supplementary analyses. RPCP was quantified both with and without large-vessel removal (RPCP/mL-RPCP), and between-group comparisons were conducted between acute NAION eyes and healthy controls using Mann–Whitney U tests. A comparison with healthy controls revealed that large vessel removal produced opposing effects on RPCP density at the VF defect region: it increased when vessels were included but

decreased after their removal (all $P < 0.05$). This allowed us to distinguish capillary-level changes from composite VD changes influenced by large-vessel signal. Furthermore, sectoral VD measurements from RPCP, SVP, ICP, and DCP were analyzed across four predefined regions (T1, T2, N1, N2). Median differences with interquartile ranges (IQRs), test statistics (Z), and *P*-values are reported in Supplementary Table S2.

Finally, to evaluate the functional relevance of vascular changes, Spearman correlation coefficients were calculated between VD parameters and visual function indices (BCVA, MD, PSD, VFI). In the acute stage, ppVD, SVP T1/N1, ICP T2/N2, and DCP T1 VD (bold values) exhibited statistically significant differences compared to HC, as well as significant correlations with visual function (all $P < 0.05$). This comprehensive mapping revealed that VD elevation was most prominent in temporal sectors (T1/T2) and correlated strongly with functional deficits, supporting our interpretation that early hyperperfusion and capillary dilation represent a true, biologically meaningful response rather than an imaging artifact.

Supplementary Table S2. Comparison of sectoral VD between acute NAION and healthy controls and Spearman correlations (r) with visual function indices

	△(Acute-HC)	*Z/t*	*P*	*r* (vision)	*P*
ppVD	**9.26[6.90,22.94]**	**-3.88**	**< 0.0001******	**BCVA = -0.52** **PSD = 0.63**	**0.02*** **0.003****
mVD	2.48[-1.03,3.08]	-1.41	0.16	MD = -0.68 PSD = 0.80 VFI = -0.49	0.02* 0.003** 0.003**
RPCP VD	13.98[9.89,14.15]	-3.70	**0.0001*****	-	-
mL RPCP VD	-2.80[-3.78,-0.42]	-2.39	**0.02***	-	-
RPCP T1 VD	1.12[0.01,1.45]	-1.67	0.09	BCVA = -0.71	0.0005***
RPCP T2 VD	0.55[-0.48,3.64]	-1.16	0.25	MD = 0.51	0.02*
RPCP N2 VD	6.07[-1.03,19.07]	-2.14	**0.03***	-	
RPCP N1 VD	-3.98[0.02,5.62]	-0.72	0.47	BCVA = -0.54 PSD = 0.77	0.01* < 0.0001****

SVP T1 VD	**5.25[1.16,5.69]**	**-2.18**	**0.03***	**PSD = 0.52**	**0.02***
SVP T2 VD	5.26[2.54,7.12]	-3.53	**0.0004*****	-	-
SVP N2 VD	-5.43[-7.50,0.50]	-1.12	0.27	BCVA = -0.62 PSD = 0.68	0.003** 0.001**
SVP N1 VD	**-1.83[-4.76,-1.74]**	**-3.07**	**0.002****	**PSD = -0.82** **VFI = 0.57**	**0.03*** **< 0.0001****
ICP T1 VD	9.22[-3.24,9.80]	-0.598	0.55	-	-
ICP T2 VD	**8.43[0.40,10.50]**	**-4.84**	**< 0.0001****	**PSD = 0.77**	**< 0.0001****
ICP N2 VD	**-2.43[-6.77,11.65]**	**-5.27**	**< 0.0001****	**PSD = 0.70**	**0.001****
ICP N1 VD	-1.06[-1.80,0.82]	-2.99	**0.003****	-	
DCP T1 VD	**1.06[-3.25,8.11]**	**-1.98**	**0.049***	**MD = -0.51** **PSD = 0.81**	**0.02*** **< 0.0001****
DCP T2 VD	1.45[-8.15,8.23]	-1.33	0.19	MD = -0.55	0.01*
DCP N2 VD	2.18[-2.36,3.54]	-0.92	0.37	-	-
DCP N1 VD	-2.48[-3.17,0.11]	-2.58	**0.01***	-	-

ppVD = peripapillary retinal vessel density, mVD = macular vessel density, RPCP = radial peripapillary capillary plexus, mL RPCP = move large vessels RPCP, SVP = superficial vascular plexus, ICP = intermediate capillary plexus, DCP = deep capillary plexus,

Bold values indicate significant acute-stage alterations relative to healthy controls were correlated with visual function. Data are presented as median [IQR]. Mann-Whitney U. $^{*}P < 0.05$, $^{**}P < 0.01$, $^{***}P < 0.001$, $^{****}P < 0.0001$.

Supplementary Quality Control of AOSLO-based RNFL Grading

To ensure the reliability of the AOSLO-derived RNFL grading system, we constructed a reference dataset with representative images for each grade. Five sample images were selected for each grade (Grade 1–3) to illustrate the defining features and to serve as a visual standard for independent rating (Supplementary Fig. S1). Two masked graders independently assessed all available images according to these predefined criteria. Interobserver agreement was evaluated using Cohen's kappa statistic, yielding ($\kappa = 0.71$, $P < 0.0001$), which indicates substantial agreement. The corresponding confusion matrix and κ statistics are provided in Supplementary Table S3. This quality control step confirmed the reproducibility and robustness of the grading system across observers.

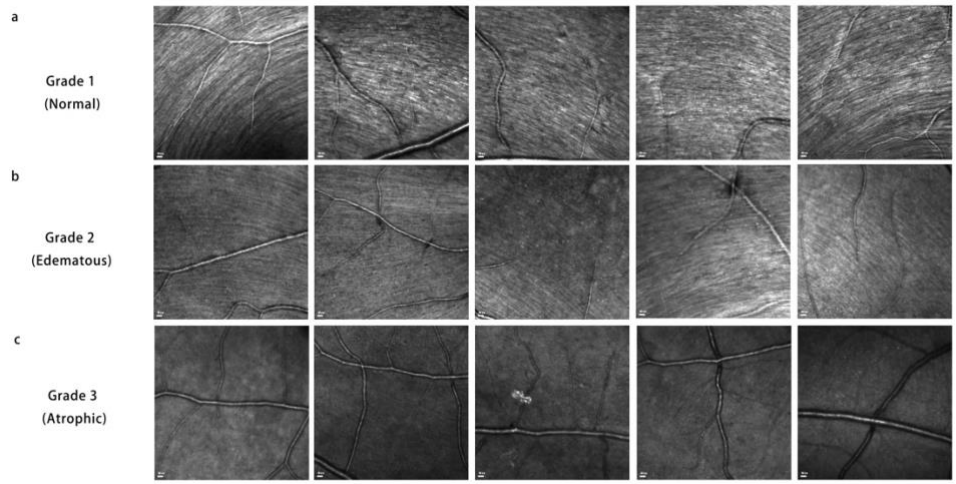

Supplementary Fig. S1 Representative examples of RNFL grading on confocal AOSLO. Each grade was illustrated by five independent samples (n = 5 eyes per grade). a Grade 1 shows regularly distributed nerve fiber bundles with intact vessel coverage. b Grade 2 demonstrates swollen and partially disorganized bundles with blurred margins. c Grade 3 reveals severely thinned, disrupted bundles with loss of vessel coverage. Images were selected as representative cases following double-masked grading by two independent examiners; discrepancies were resolved by consensus. Scale bar = 50μm.

Supplementary Table S3. Confusion matrix for AOSLO-RNFL grading (Observer A × Observer B).

		Observer B			
		Grade1	Grade2	Grade3	Row total
Observer A	Grade1	18	2	0	20
	Grade2	3	19	2	24
	Grade3	0	2	23	25
	Column total	21	23	25	69

Unweighted Cohen's kappa = 0.71, $P < 0.0001$; Overall percent agreement = 86%.

Discrepant cases (n = 69) were resolved by consensus adjudication.

Confocal AOSLO reveals hyperreflective dot-like foci (HDF) infiltration in 8 acute NAION eyes:

HDF clusters appeared as white, dot-like structures as discrete, round or oval hyperreflective structures with suspected pseudopodia located in the RNFL layer, with radial arrangements and were observed in 8 acute cases (Supplementary Fig. S2 and Table S4).

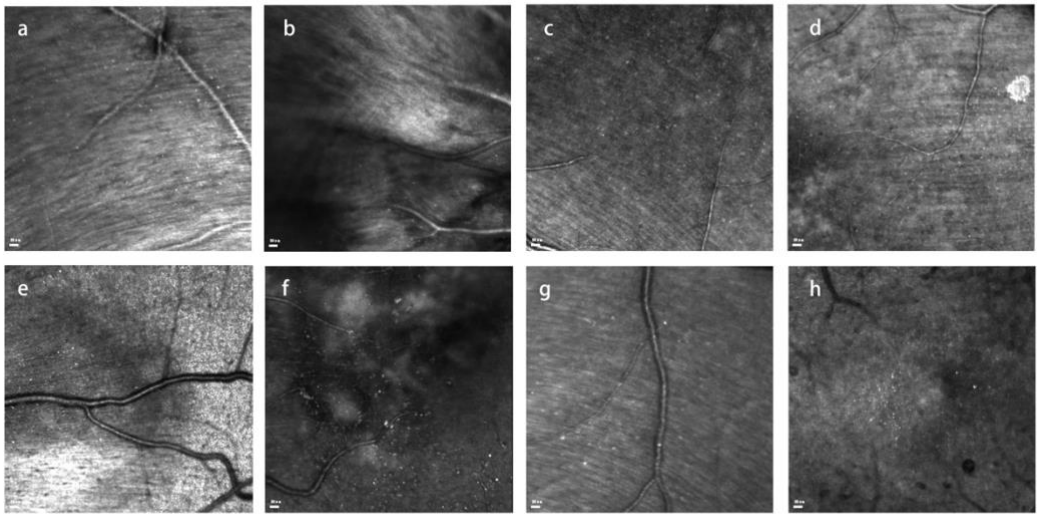

Supplementary Fig. S2 a-h Representative AOSLO images showing hyperreflective dot-like foci (arrows) localized adjacent to swollen RNFL bundles in acute NAION eyes. These punctate aggregates were observed in 8/22 acute eyes, typically within the first week after onset. Scale bar = 50 μm.

Supplementary Table S4. Confusion matrix for AOSLO- HDF infiltration (Observer A × Observer B).

		Observer B		
		HDF(+)	HDF(-)	Row total
Observer A	HDF(+)	8	2	10
	HDF(-)	1	11	12
	Column total	9	13	22

Unweighted Cohen's kappa = 0.72, $P < 0.001$; Overall percent agreement = 86%.
Discrepant cases ($n = 22$) were resolved by consensus adjudication.

At the acute stage, when patients were stratified according to HDF infiltration, no significant differences were observed between HDF+ and HDF- eyes in terms of BCVA (logMAR: $P = 0.57$), MD ($P = 0.76$), PSD ($P = 0.82$), VFI ($P = 0.97$), pRNFLT ($P = 0.40$), GCIPLT ($P = 0.99$), or in any of the sectoral thickness parameters (all $P > 0.05$). These results indicate that acute-phase structural and functional parameters are not significantly influenced by the presence or absence of HDF involvement, supporting the notion that functional and vascular alterations may precede measurable macular structural

differences in NAION (Supplementary Table S5).

Supplementary Table S5 Comparisons of visual function and structural parameters between NAION eyes with and without HDF

Characteristic Acute stage	HDF+ (n = 8)	HDF- (n = 14)	Z	P-value
BCVA, logMAR	0.37[0.03,0.79]	0.22[0.00,0.57]	-0.62	0.57
MD, dB	-10.09[-11.58,-5.055]	-9.80[-10.79,-4.71]	-0.34	0.76
PSD, dB	8.91[5.12,11.39]	10.14[4.82,11.67]	-0.28	0.82
VFI, %	76[66,86]	78[61,88]	-0.07	0.97
pRNFLT	299.50[222.00,374.50]	339.00[260.00,379.00]	-0.89	0.40
GCIPLT	73.03[71.13,79.00]	74.34[69.95,80.55]	0.00	1.00
S3vsI3	33.07[29.95,38.53]	33.81[32.33,39.97]	-0.59	0.57
S6vsI6	52.67[47.20,56.00]	52.67[49.03,53.33]	-0.03	0.97
S9vsI9	67.46[58.11,90.08]	71.80[61.35,90.34]	-0.41	0.71
S12vsI12	62.11[60.88,69.13]	61.61[61.08,65.68]	-0.10	0.92
T1	63.17[59.02,64.52]	62.35[56.73,64.70]	-0.42	0.71
T2	76.31[72.35,78.87]	76.69[71.35,78.87]	-0.07	0.97
N2	85.60[78.35,89.13]	85.25[76.17,89.15]	-0.14	0.92
N1	87.82[84.26,92.36]	87.82[85.56,93.82]	-0.35	0.76

HDF^+ = eyes with hyperreflective dot-like structures foci involvement; HDF^- = eyes without hyperreflective dot-like structures foci involvement.

Data are presented as median [IQR]. Mann-Whitney U. $^{*}P < 0.05$, $^{**}P < 0.01$, $^{***}P < 0.001$, $^{****}P < 0.0001$.